

## Many-body effects in the electromodulation spectra of modulation-doped quantum wells: Theory and experiment

Godfrey Gumbs\* and Danhong Huang

*Department of Physics and Astronomy, Hunter College, City University of New York,  
695 Park Avenue, New York, New York 10021*

Yichun Yin,\* H. Qiang, D. Yan, and Fred H. Pollak\*

*Department of Physics, Brooklyn College, City University of New York, Brooklyn, New York 11210*

Thomas F. Noble

*Materials Science and Engineering Department, Johns Hopkins University, Baltimore, Maryland 21218*

(Received 1 September 1993)

We have performed a theoretical (first-principles) and experimental (contactless electroreflectance) investigation of the temperature dependence ( $17 < T < 351$  K) of the electric-field-modulated interband transitions in a pseudomorphic  $\text{Ga}_{0.81}\text{Al}_{0.19}\text{As}/\text{In}_{0.20}\text{Ga}_{0.80}\text{As}/\text{GaAs}$  modulation-doped quantum well that contains a two-dimensional electron gas. We find that many-body effects are a factor at all temperatures although they are most pronounced for  $T \leq 152$  K. Because of the derivativelike nature of our approach, both theoretical and experimental, the weak Fermi-edge transition is still visible up to at least 152 K, as a complement to the results of previous theoretical and experimental investigations.

Modulation-doped quantum-well (MDQW) structures containing a two-dimensional electron gas (2D EG) have recently attracted a great deal of attention both for fundamental physics as well as for device applications. These systems possess unique properties for the study of many important physical phenomena such as the Fermi-edge singularity due to electron-hole multiple scattering,<sup>1-3</sup> quenching of excitons due to phase-space filling and screening,<sup>1-6</sup> the Burstein-Moss shift due to band filling,<sup>1-3,7</sup> etc. Furthermore, such structures also form the basis for high electron mobility transistors (HEMT's) which are believed to have superior performance over other solid-state amplifiers or receivers at frequencies up to 100 GHz.<sup>8-10</sup> One of these transistors is the pseudomorphic  $\text{Ga}_{1-y}\text{Al}_y\text{As}/\text{In}_x\text{Ga}_{1-x}\text{As}/\text{GaAs}$  MDQW, which has exhibited outstanding power performance. The large  $\text{Ga}_{1-y}\text{Al}_y\text{As}/\text{In}_x\text{Ga}_{1-x}\text{As}$  conduction-band discontinuity allows high 2D EG densities ( $n_{2D}$ ) in the  $\text{In}_x\text{Ga}_{1-x}\text{As}$  channel.

In spite of the proven utility of modulation spectroscopy in studying semiconductor microstructures,<sup>11,12</sup> relatively little work has been done on 2D EG systems.<sup>12</sup> Modulation spectroscopy studies of  $\text{Ga}_{1-y}\text{Al}_y\text{As}/\text{GaAs}$  modulation-doped heterojunctions (MDHJ's) (and  $\delta$ -doped GaAs) have not shown clear evidence for a signature associated with the 2D EG and have been the subject of considerable controversy.<sup>11,13</sup> This is because in these systems the observed signals in the spectral vicinity of the direct band gap of GaAs could originate in either the 2D EG (in the "triangular"-shaped potential at the  $\text{GaAs}/\text{Ga}_{1-y}\text{Al}_y\text{As}$  interface) or in other GaAs portions of the sample. This problem has been averted by studying  $\text{Ga}_{1-y}\text{Al}_y\text{As}/\text{In}_x\text{Ga}_{1-x}\text{As}/\text{GaAs}$  MDQW systems since in this case the 2D EG signature will be associated with the  $\text{In}_x\text{Ga}_{1-x}\text{As}$  section of the sample, which is spectrally separated from the GaAs and  $\text{Ga}_{1-y}\text{Al}_y\text{As}$  signals.<sup>5,6</sup>

Using photoreflectance and electroreflectance, Yin

*et al.* have investigated both  $\delta$ -doped<sup>5</sup> and step-doped<sup>6</sup>  $\text{Ga}_{1-y}\text{Al}_y\text{As}/\text{In}_x\text{Ga}_{1-x}\text{As}/\text{GaAs}$  structures with different material parameters. In their previous works, the spectra from the  $\text{In}_x\text{Ga}_{1-x}\text{As}$  MDQW channel have been accounted for on the basis of a simple one-electron line shape, i.e., the first derivative of a broadened steplike 2D density of states and a Fermi-level filling factor.<sup>5,6</sup> A detailed fit of this function to the experimental data makes it possible to evaluate the Fermi energy ( $E_F$ ), and hence  $n_{2D}$ . Furthermore, other important parameters of the system such as built-in electric fields, In composition, and well width ( $L$ ) of the  $\text{In}_x\text{Ga}_{1-x}\text{As}$  MDQW channel can be evaluated.<sup>5,6</sup> However, the simple one-electron fit to the spectra is found to be good only for data taken at high temperatures ( $T > 152$  K), for which many-body effects are small.

We have recently observed that for  $T \leq 152$  K the derivative contactless electroreflectance (CER) (Ref. 14) trace contains a high-energy peak, related to the Fermi-edge transition, which exhibits strong many-body effects. The derivative nature of modulation spectroscopy makes it possible to observe such Fermi-edge features at temperatures considerably higher than other optical methods.<sup>1-4,7</sup> Therefore, for such 2D EG systems it is important to have a general theory of the temperature dependence of the electromodulation spectra which includes many-body effects.

The hole created by the photoexcitation of an electron in the valence band may be used to probe the equilibrium properties of electron systems. The creation of a photoexcited hole also introduces a finite perturbation to the initial equilibrium state of electron systems. This has been of interest from both a theoretical and an experimental point of view.<sup>3,15,16</sup> This problem was considered theoretically by Mahan<sup>17</sup> for electron-hole scattering. Subsequent theoretical work included the dynamical screening of the Fermi sea, as well as effects due to exchange arising from an increased carrier density.<sup>18,19</sup> As

a result of excitonic many-body effects, an enhancement of the absorption at the Fermi edge was obtained. This many-particle excitonic feature is actually composed of two compensating processes, i.e., the scattering of electrons by holes (vertex correction) and the strong renormalization of the electron self-energy.<sup>15,16,20</sup> The appreciable exciton enhancement was shown to survive in the low-temperature regime ( $T \leq 50$  K).<sup>2</sup> However, in our derivative CER experiment the Fermi-edge transition is actually observed to temperatures as high as 152 K.

In this paper, we now present the general formulation for the absorption of light, and its derivative, by a MDQW. These results are in excellent agreement with a CER experiment on a  $\text{Ga}_{0.81}\text{Al}_{0.19}\text{As}/\text{In}_{0.20}\text{Ga}_{0.80}\text{As}/\text{GaAs}$  HEMT structure in the temperature range  $17 < T < 351$  K, including the observation of the Fermi-edge transition at temperatures up to 152 K. The details are given by the description for sample No. 1 in Ref. 6. The theory also has important ramifications for the optical and modulated optical studies of other 2D EG systems such as  $\text{GaAs}/\text{Ga}_{1-y}\text{Al}_y\text{As}$ ,<sup>4</sup>  $\text{Ga}_{1-y}\text{In}_y\text{As}/\text{Al}_{1-x}\text{In}_x\text{As}$ ,<sup>7</sup> and  $\text{In}_x\text{Ga}_{1-x}\text{As}/\text{InP}$  (Ref. 1) MDQW's. Therefore, it is now possible to correlate the line shapes of modulation experiments in these systems with a first-principles theory rather than the phenomenological expression used in the past.<sup>5,6</sup> This comparison results in the understanding of new phenomena, such as the high-temperature behavior of the Fermi-edge transition, and in greater confidence in the obtained relevant parameters such as  $n_{2D}$ .

In our approach, the interactions between the electrons in the Fermi sea and the electron-hole pairs as well as the coupling between excitons are included. The absorption of light for interband transitions at temperature  $T$  can be written as<sup>17</sup>

$$\text{Re}\alpha(\omega) = \frac{e^2\beta^2\omega}{\pi\epsilon_0 L n(\omega)} [\rho_{\text{ph}}(\omega) + 1] S(\omega), \quad (1)$$

$$V_{m'n',mn}(\omega) = -\frac{2\pi e^2}{\epsilon_s(\omega)} \int_{-\infty}^{\infty} dz \int_{-\infty}^{\infty} dz' \xi_m^c(z') \xi_n^{\text{HH}}(z') |z - z'| \xi_m^c(z) \xi_n^{\text{HH}}(z). \quad (7)$$

The phonon coupling is included through a frequency-dependent dielectric function  $\epsilon_s(\omega) = \epsilon_b [\omega^2 - \omega_{\text{LO}}^2 + i\gamma_{\text{ph}}\omega] / [\omega^2 - \omega_{\text{TO}}^2 + i\gamma_{\text{ph}}\omega]$ , where  $\gamma_{\text{ph}}$  is a phonon broadening parameter,  $\omega_{\text{LO}}$  and  $\omega_{\text{TO}}$  are the longitudinal and transverse optical-phonon frequencies, and  $\epsilon_b \equiv 4\pi\epsilon_0\epsilon_{\infty}$ . When the exciton coupling is neglected, the response function at finite temperature has been calculated as

$$\chi_{mn}^{(0)}(\omega) = \frac{1}{2\pi} \int_0^{\infty} dk^2 [f_0(E_m^{\text{HH}}(k^2)) - f_0(E_n^c(k^2))] \Gamma_{mn}(k, \omega) \left[ \frac{1}{\hbar\omega - E_{mn}(k^2) + i\hbar/\tau_{mn}} - \frac{1}{\hbar\omega + E_{mn}(k^2) + i\hbar/\tau_{mn}} \right]. \quad (8)$$

Here,  $E_{mn}(k^2) \equiv E_n^c(k^2) - E_m^{\text{HH}}(k^2)$ , and  $\hbar/\tau_{mn}$  is the broadening due to impurities, density fluctuations in the alloy composition, and interface imperfection. The Fermi function is  $f_0(E)$  with Fermi energy  $E_F$  determined from the fixed electron density  $n_{2D}$ . In a MDQW, the exciton interaction is strong, the hole density is low, and the range of the exciton interaction is short due to the screening from the other electrons in the well. Under these conditions, the ladder approximation can be used to

$$n(\omega) = \sqrt{\epsilon_{\infty}} - \frac{e^2\alpha^2}{2\pi\epsilon_0 L \sqrt{\epsilon_{\infty}}} [\rho_{\text{ph}}(\omega) + 1] \times \sum_{\nu, \nu'} B_{\nu, \nu'} [\text{Re}Q_{\nu, \nu'}(\omega)], \quad (2)$$

where  $\rho_{\text{ph}}(\omega) = 1/[e^{\hbar\omega/k_B T} - 1]$  is the photon distribution function.  $S(\omega)$ , the dynamical structure factor, which includes all the optical responses from the electron system and the coupling between the transitions, is

$$S(\omega) = \sum_{\nu, \nu'} B_{\nu, \nu'} [-\text{Im}Q_{\nu, \nu'}(\omega)]. \quad (3)$$

The screened response function  $Q_{\nu, \nu'}(\omega)$  in the presence of exciton couplings is the solution of the Dyson equation and is given by

$$Q_{\nu, \nu'}(\omega) = \epsilon_{\nu\nu'}^{-1}(\omega) \chi_{\nu}^{(0)}(\omega), \quad (4)$$

where  $\chi_{\nu}^{(0)}(\omega)$  is the response function for uncoupled excitons, and  $\epsilon_{\nu\nu'}^{-1}(\omega)$  is the inverse dielectric function matrix for exciton coupling. Also,  $B_{\nu, \nu'}$  is a form factor which determines the peak strength of the absorption in the spectrum and is calculated from<sup>21</sup>

$$B_{\nu, \nu'} = \int_{-\infty}^{\infty} dz \int_{-\infty}^{\infty} dz' \xi_m^c(z) \xi_n^{\text{HH}}(z) \xi_m^c(z') \xi_n^{\text{HH}}(z'). \quad (5)$$

In Eq. (1),  $\beta = |\langle u_c(\mathbf{r}) | \mathbf{r} | u_v(\mathbf{r}) \rangle|$  is the dipole matrix element<sup>21</sup> for the Bloch state  $u_c(\mathbf{r})$  of an electron in the conduction band and the Bloch state  $u_v(\mathbf{r})$  of an electron in the valence band,  $\epsilon_{\infty}$  is the optical dielectric constant of the well material,  $L$  is the well width, and  $\omega$  is the frequency of the incident light. In our notation,  $\nu = (m, n)$  is a composite index labeling the valence and conduction subbands.

In the generalized random-phase approximation, the dielectric function is of the form

$$\epsilon_{m'n',mn}(\omega) = \delta_{m'm} \delta_{n'n} - \chi_{m'n'}^{(0)}(\omega) V_{m'n',mn}(\omega), \quad (6)$$

where the coupling matrix element between different types of excitons is given by

include the vertex correction  $\Gamma_{mn}(k, \omega)$  to the response function in Eq. (8).<sup>17,18</sup> The Bethe-Salpeter equation for  $\Gamma_{mn}(k, \omega)$  is solved by casting it into a linear matrix equation associated with the discrete values of the wave vector  $k$ . The cutoff value we use for  $k$  is an order of magnitude larger than the Fermi wave vector. The Thomas-Fermi model is used for the static shielding of the exciton interaction. The band edges  $E_n^c, E_m^{\text{HH}}$  and the envelope functions  $\xi_n^c(z), \xi_m^{\text{HH}}(z)$  are calculated by using the self-

consistent Hartree approximation.<sup>22</sup>

In our numerical calculations, the energy dispersion relation for electrons is parabolic. The energy dispersion relation for holes, which was taken from a  $\mathbf{k}\cdot\mathbf{p}$  theory,<sup>21</sup> includes the splitting, coupling, and nonparabolic effects on the light- and heavy-hole subbands. The parameters used in our calculations are as follows:  $L = 100 \text{ \AA}$ ,  $\hbar\omega_{\text{LO}} = 36.7 \text{ meV}$ ,  $\hbar\omega_{\text{TO}} = 33.6 \text{ meV}$ ,  $\epsilon_{\infty} = 11.587$ ,  $n_{2\text{D}} = 1.9 \times 10^{12} \text{ cm}^{-2}$ ,  $\hbar\gamma_{\text{ph}} = 5 \text{ meV}$ , and the energy shift due to strain is taken as  $S_1 = 89.6 \text{ meV}$ . For this system,  $E_F$  lies between the first and second electron subbands. The broadening can affect the derivative of the absorption spectrum. We have adjusted the broadening parameters  $\hbar/\tau_{mn}$  to fit our numerical results to the experimental data. We choose four broadening parameters to fit the spectrum at high temperature  $T = 351 \text{ K}$  from a single-particle model. We found that the line shape is not very sensitive to small changes (a few meV) in these parameters.

Plotted in Fig. 1 is the derivative of the absorption (in units of  $\alpha_0 = e^2\beta^2/\hbar c\epsilon_0 L^3\sqrt{\epsilon_{\infty}}$ ) with respect to the frequency of the incident light. It is plotted as a function of the photon energy,  $\hbar\omega$ , for  $T = 351, 152, 80,$  and  $17 \text{ K}$ . At the lowest temperature (solid line), the transition 21HH is very intense compared to the other peaks in the spectrum. The notation  $mn\text{HH}$  denotes a transition from the  $m$ th conduction to the  $n$ th valence subband of heavy-hole (HH) character. For the sake of clarity (a) the zero of energy is taken to be  $E_{21\text{HH}}$ , the energy of the transition from the first HH subband to the second electron subband, and (b) the curves are displaced. The strength of 21HH is due to the strong mixing of the symmetric and antisymmetric states by the built-in electric field which results from the asymmetry of the doping and the quantum-well structure. The strength of the 22HH tran-

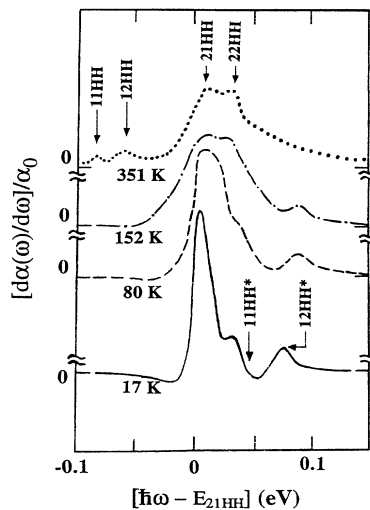


FIG. 1. Calculated derivative of the absorption strength, in units of  $\alpha_0$ , as a function of the photon energy measured from  $E_{21\text{HH}}$ . In this figure, the solid line is for  $T = 17 \text{ K}$ , the dashed line is for  $T = 80 \text{ K}$ , the dash-dot line is for  $T = 152 \text{ K}$ , and the dotted line is for  $T = 351 \text{ K}$ . The peak with the highest energy at  $T = 17 \text{ K}$  is related to the Fermi-edge transitions. The notations  $mn\text{HH}$  and  $mn\text{HH}^*$  are defined in the text.

sition, at energy  $E_{22\text{HH}}$ , is greatly reduced. Furthermore, due to the occupation of the first electron subband at low temperatures, we are not able to see transitions that go to that subband from the first and second HH subbands, i.e., 11HH and 12HH.

The steps in the absorption spectrum, corresponding to the band-edge transitions, give the peaks in the derivative spectrum, while the absorption peaks arising from the Fermi-edge transitions produce the sign changes in the derivative of the absorption coefficient. The zero in the derivative spectrum corresponds to the peak positions in the absorption coefficient. We denote it by 11HH\* for the Fermi-edge transition from the first HH level to the first electron subband.<sup>1,2</sup> On the other hand, another Fermi-edge transition 12HH\* only shows a step in the absorption spectrum because there is no sign change in the derivative with respect to it.

The observed Fermi-edge transitions, 11HH\* and 12HH\*, are a result of enhanced many-body effects and the formation of excitons. Our numerical calculations show that the excitonic interaction between electrons and holes plays a key role in this enhancement. The binding energy of an exciton is estimated as  $\sim 10 \text{ meV}$  at low temperature. The electron-electron interaction in the degenerate Fermi sea strongly correlates these excitons and greatly affects the line shape of this peak. Moreover, the coupling between excitons shifts this peak. When  $T = 80 \text{ K}$  (dashed line), both the transitions of 22HH and 11HH\* are almost suppressed, but the other Fermi-edge transition 12HH\* is still visible up to  $T = 152 \text{ K}$  (see the dotted-dashed line). The visible Fermi-edge transition at high temperature can only have a step, and not a peak, in the absorption spectrum since it does not have a negative derivative. This complements the results based on the previous model<sup>2</sup> where the Fermi-edge enhancement in the absorption spectrum only survives up to  $T = 50 \text{ K}$ . Our numerical calculations are supported by the experimental data, as will be discussed below. The negative derivative of the absorption spectrum at low temperatures is from the contribution of  $dn(\omega)/d\omega$  in Eq. (2).

For a high temperature of  $T = 351 \text{ K}$  (dotted line in Fig. 1), the Fermi-edge transition is completely suppressed. However, there are two features arising from the 11HH and 12HH transitions at energies  $E_{11\text{HH}}$  and  $E_{12\text{HH}}$ , respectively. The thermal broadening line shape of these two peaks depends sensitively on  $E_F$  and the temperature, thus providing us with a tool to evaluate  $E_F$  from a detailed line-shape fit. In this way, we are able to determine  $n_{2\text{D}}$  within the quantum well. We also found a small blueshift for the peak 21HH for the increased temperature. The strength of the 22HH peak increases with elevated temperatures and becomes as strong as 21HH at high temperatures (152–351 K).

In Fig. 2, the experimental CER data from sample No. 1 in Ref. 6 for  $T = 17, 80, 152,$  and  $351 \text{ K}$  are presented as a comparison with our calculations. At the highest temperature, two weak and two strong features are observed from the  $\text{In}_x\text{Ga}_{1-x}\text{As}$  MDQW. These have been identified as 11HH, 12HH, 21HH, and 22HH, respectively.<sup>6</sup> The peak labeled  $E_0(\text{GaAs})$  corresponds to the direct gap of GaAs and originates in the GaAs

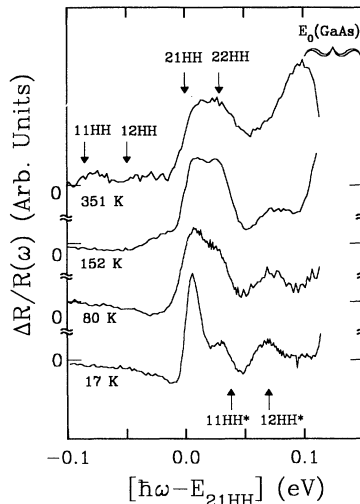


FIG. 2. Experimental CER data as a function of the photon energy measured from  $E_{21HH}$ . The measurements are in the temperature regime between  $T=17$  and 351 K.

buffer/substrate. Again, for the sake of clarity (a) the zero of energy is taken to be  $E_{21HH}$  and (b) the curves are displaced. As the temperature is lowered, 11HH and 12HH disappear and a resonance denoted 12HH\* becomes evident at  $T=152$  K. There is very good agreement between theory and experiment at both high and low temperatures. Many of the observed features are reproduced in our theory including the absorptive peaks to the first occupied electron subband (11HH and 12HH) at elevated temperatures, the temperature dependence of the strongest peak (21HH), and the 22HH structure as well as the Fermi-edge transitions (11HH\*, 12HH\*) up to 152 K. There are some changes in the widths of the spectral features as a result of the temperature dependence of the phonon broadening.

Even for temperatures as high as  $T=351$  K, where many-body effects are expected to be small, we still observe an appreciable modification to the simplified single-electron model. Although there is no shift in the peak position for the band-edge transitions, we obtain an appreciable shift for the Fermi-edge transitions at low temperature. This relative change is largely independent of the details of the model, but it illustrates the importance of the many-body corrections. We also find the relationship between the cusps in the absorption spectrum and the peaks in its derivative. The features in the absorption spectrum are significantly amplified, which gives a very accurate determination of the Fermi energy by fitting the thermally broadened line shape.

In conclusion, we have performed a detailed first-principles theoretical and experimental CER investigation of the temperature dependence ( $17 < T < 351$  K) of the modulated interband transitions in a pseudomorphic  $\text{Ga}_{0.81}\text{Al}_{0.19}\text{As}/\text{In}_{0.20}\text{Ga}_{0.80}\text{As}/\text{GaAs}$  modulation-doped quantum well that contains a 2D EG. We find that many-body effects are a factor at all temperatures although they are most pronounced for  $T \leq 152$  K. Because of the derivativelike nature of our approach, both theoretical and experimental, the Fermi-edge transition is still visible up to at least 152 K, a complement to previous works. There is very good agreement between theory and experiment. Therefore, it is now possible to compare the line shapes of modulation experiments in these systems with a first-principles theory rather than the phenomenological expressions used in the past, resulting in greater confidence in the obtained relevant parameters such as  $n_{2D}$ .

The authors gratefully acknowledge the support in part from the City University of New York PSC-CUNY-BHE Grants No. 662505 and No. 664239, the Olympus Corporation, and NSF Grant No. DMR-9120363.

\*Also at The Graduate School and University Center, City University of New York, 33 West 42 Street, New York, NY 10036.

<sup>1</sup>S. Schmitt-Rink, D. S. Chemla, and D. A. B. Miller, *Adv. Phys.* **38**, 89 (1989).

<sup>2</sup>G. Livescu *et al.*, *IEEE J. Quantum Electron.* **24**, 1677 (1988).

<sup>3</sup>W. Chen *et al.*, *Phys. Rev. B* **45**, 8464 (1992).

<sup>4</sup>D. Huang *et al.*, *Phys. Rev. B* **38**, 1246 (1988).

<sup>5</sup>Y. Yin *et al.*, *Appl. Phys. Lett.* **61**, 1579 (1992); also, *Proc. SPIE* **1675**, 408 (1992).

<sup>6</sup>Y. Yin, H. Qiang, D. Yan, F. H. Pollak, and T. F. Noble, *Semicond. Sci. Technol.* **8**, 1599 (1993).

<sup>7</sup>Y.-H. Zhang and K. Ploog, *Phys. Rev. B* **45**, 14069 (1992).

<sup>8</sup>See, for example, P. M. Smith, P. C. Chao, J. M. Ballingall, and A. W. Swanson, *Microwave J.* **33**, 71 (1990).

<sup>9</sup>See, for example, H. Morkoc and H. Unlu, in *Semiconductors and Semimetals*, edited by R. Dingle (Academic, New York, 1987), Vol. 24, p. 135.

<sup>10</sup>See, for example, W. J. Schaff, P. J. Tasker, M. C. Foisy, and L. F. Eastman, in *Semiconductors and Semimetals*, edited by T. P. Pearsall (Academic, New York, 1990), Vol. 33, p. 73.

<sup>11</sup>F. H. Pollak and H. Shen, *Mater. Sci. Eng.* **R10**, 375 (1993).

<sup>12</sup>O. J. Glembocki and B. V. Shanabrook, in *Semiconductors and Semimetals*, edited by D. G. Seiler and C. L. Littler (Academic, New York, 1992), Vol. 67, p. 222.

<sup>13</sup>See, for example, N. Pan, X. L. Zheng, H. Hendriks, and J. Carter, *J. Appl. Phys.* **68**, 2355 (1990).

<sup>14</sup>Y. Yin and F. H. Pollak, *Appl. Phys. Lett.* **59**, 2305 (1991).

<sup>15</sup>P. Hawrylak, *Phys. Rev. B* **42**, 8986 (1990); **44**, 6262 (1991); **45**, 4237 (1992).

<sup>16</sup>A. E. Ruckenstein, and S. Schmitt-Rink, *Phys. Rev. B* **35**, 7551 (1987); J. F. Mueller, A. E. Ruckenstein, and S. Schmitt-Rink, *Mod. Phys. Lett. B* **2**, 35 (1991).

<sup>17</sup>G. D. Mahan, *Phys. Rev.* **153**, 8822 (1967).

<sup>18</sup>G. D. Mahan, *Phys. Rev. B* **21**, 1421 (1980).

<sup>19</sup>P. Nozières and C. T. De Dominicis, *Phys. Rev.* **178**, 1097 (1969).

<sup>20</sup>S. Schmitt-Rink, C. Ell, and H. Haug, *Phys. Rev. B* **33**, 1183 (1983).

<sup>21</sup>G. Bastard and J. A. Brum, *IEEE J. Quantum Electron.* **QE-22**, 1625 (1986).

<sup>22</sup>T. Ando, *Phys. Rev. B* **13**, 3468 (1976); **59**, 2305 (1991).